AMERICAN SOCIETY FOR MICROBIOLOGY | Applied and Environmental Microbiology®

Identification of the *hcb* Gene Operon Involved in Catalyzing Aerobic Hexachlorobenzene Dechlorination in *Nocardioides* sp. Strain PD653

Koji Ito,[a,b] Kazuhiro Takagi,[a,b] Akio Iwasaki,[c] Naoto Tanaka,[a] Yu Kanesaki,[d] Fabrice Martin-Laurent,[e] Shizunobu Igimi[a]

Department of Agricultural Chemistry, Tokyo University of Agriculture, Tokyo, Japan[a]; Hazardous Chemicals Division, Institute for Agro-Environmental Sciences, NARO, Kannondai, Tsukuba-shi, Ibaraki, Japan[b]; Clinical Research Support Center, Juntendo University, Hongo, Tokyo, Japan[c]; Genome Research Center, NODAI Research Institute, Tokyo University of Agriculture, Tokyo, Japan[d]; UMR AgroEcologie, INRA, AgroSup Dijon, University Bourgogne Franche-Comté, Dijon, France[e]

ABSTRACT *Nocardioides* sp. strain PD653 was the first identified aerobic bacterium capable of mineralizing hexachlorobenzene (HCB). In this study, strain PD653-B2, which was unexpectedly isolated from a subculture of strain PD653, was found to lack the ability to transform HCB or pentachloronitrobenzene into pentachlorophenol. Comparative genome analysis of the two strains revealed that genetic rearrangement had occurred in strain PD653-B2, with a genomic region present in strain PD653 being deleted. *In silico* analysis allowed three open reading frames within this region to be identified as candidate genes involved in HCB dechlorination. Assays using recombinant *Escherichia coli* cells revealed that an operon is responsible for both oxidative HCB dechlorination and pentachloronitrobenzene denitration. The metabolite pentachlorophenol was detected in the cultures produced in the *E. coli* assays. Significantly less HCB-degrading activity occurred in assays under oxygen-limited conditions ($[O_2] < 0.5$ mg liter^{-1}) than under aerobic assays, suggesting that monooxygenase is involved in the reaction. In this operon, *hcbA1* was found to encode a monooxygenase involved in HCB dechlorination. This monooxygenase may form a complex with the flavin reductase encoded by *hcbA3*, increasing the HCB-degrading activity of PD653.

IMPORTANCE The organochlorine fungicide HCB is widely distributed in the environment. Bioremediation can effectively remove HCB from contaminated sites, but HCB-degrading microorganisms have been isolated in few studies and the genes involved in HCB degradation have not been identified. In this study, possible genes involved in the initial step of the mineralization of HCB by *Nocardioides* sp. strain PD653 were identified. The results improve our understanding of the protein families involved in the dechlorination of HCB to give pentachlorophenol.

KEYWORDS HCB, *Nocardioides* sp. strain PD653, aerobic dechlorination, monooxygenase

Received 10 April 2017 **Accepted** 11 July 2017

Accepted manuscript posted online 21 July 2017

Citation Ito K, Takagi K, Iwasaki A, Tanaka N, Kanesaki Y, Martin-Laurent F, Igimi S. 2017. Identification of the *hcb* gene operon involved in catalyzing aerobic hexachlorobenzene dechlorination in *Nocardioides* sp. strain PD653. Appl Environ Microbiol 83:e00824-17. https://doi.org/10.1128/AEM.00824-17.

Editor Ning-Yi Zhou, Shanghai Jiao Tong University

Address correspondence to Kazuhiro Takagi, ktakagi@affrc.go.jp.

A wide range of halogenated organic compounds have been used in different applications. Hexachlorobenzene (C_6Cl_6; HCB) is an organochlorine fungicide that has been used worldwide since the 1940s (1). The use of HCB was discontinued in many countries in the 1970s because of its toxicity and environmental persistence, and it was classed as a persistent organic pollutant at the Stockholm Convention in 2001. However, HCB remains a widely distributed environmental contaminant.

Bioremediation is a microorganism-based approach to remediating contaminated

sites. Bioremediation is expected to be an effective way of removing pollutants, including persistent organic pollutants, from contaminated environments. However, heavily halogenated organic compounds are less biodegradable than are many other organic compounds. Microorganisms capable of degrading HCB have been isolated and identified in few studies.

There have been many insights into the bacterium-driven reductive dehalogenation of HCB. *Dehalococcoides* sp. strain CBDB1 is one of the most extensively studied anaerobic bacteria capable of dechlorinating HCB (2, 3). Strain CBDB1 uses polychlorinated benzenes as growth-supporting electron acceptors, and dechlorinates HCB through organohalide respiration; the end products have been found to be 1,3,5-trichlorobenzene, 1,3-dichlorobenzene, and 1,4-dichlorobenzene (4). This strain also dechlorinates pentachlorobenzene (4), 1,2,3-trichlorobenzene, 1,2,4-trichlorobenzene, all of the tetrachlorobenzene isomers (5), and polychlorinated phenols (6). The chlorobenzene reductive dehalogenase gene *cbrA* was recently identified (7). Strain CBDB1 has been studied biochemically, and the complete genome has been sequenced and 32 reductive dehalogenase homologs identified (8). Sequencing *Dehalococcoides* genomes will provide additional insights into polychlorinated benzene biodegradation under anaerobic conditions.

The biodegradation of HCB under strictly aerobic conditions has been described in few publications. To the best of our knowledge, only a genetically engineered mutant of CYP101 ($P450_{cam}$) has been found to aerobically dehalogenate HCB to give pentachlorophenol (PCP) (9). The reaction is catalyzed by a two-component monooxygenase formed by a putidaredoxin reductase, PdR, that transfers an electron from the NADH cofactor to terminal oxygenase CYP101. Analysis of the three-dimensional structure of the mutant demonstrated the importance of the L244A mutation, which improves the catalytic site by making space for pentachlorobenzene and HCB chlorine atoms (10). An engineered *Sphingobium chlorophenolicum* ATCC 32723 with a gene cassette (*camA*$^+$ *camB*$^+$ *camC*) encoding the F87W/Y96F/L244A/V247L cytochrome $P\text{-}450_{cam}$ variant has been found to degrade HCB without toxic intermediates accumulating (11).

The metabolism of HCB by naturally occurring bacteria under aerobic conditions has been studied. Liu et al. found that the genera *Azospirillum* and *Alcaligenes* were dominant members of a HCB-using community isolated from contaminated soil (12). *Nocardioides* sp. strain PD653 was the first bacterium capable of mineralizing HCB under aerobic conditions that was identified (13). This strain was isolated from an upland soil contaminated with pentachloronitrobenzene (PCNB), and it was found to degrade both PCNB and HCB. The proposed HCB metabolic pathway in strain PD653 is shown in Fig. 1A. Strain PD653 mineralizes HCB via PCP. The intermediate metabolites tetrachlorohydroquinone (TeCH) and 2,6-dichlorohydroquinone (DiCH) have also been detected. Various bacteria degrade PCP (14–18). The genes encoding enzymes involved in PCP degradation by *Sphingobium chlorophenolicum* ATCC 39723 have been elucidated in detail (19). However, the gene encoding the dehalogenase involved in the first step of aerobic HCB dechlorination remains unidentified.

In this study, strain PD653-B2, which was found to have lost the ability to transform HCB into PCP, was isolated and characterized. Comparing the PD653 and PD653-B2 draft genomes allowed a genomic region that had been deleted in the derivative strain to be identified. This region was found to contain genes specific to the native PD653 strain. Heterologous expression in *Escherichia coli* revealed that the genes encode HCB-oxidative dehalogenase components.

RESULTS

Ability of strain PD653-B2 to catabolize HCB and PCP. We isolated *Nocardioides* sp. strain PD653-B2 (GenBank accession number LC196157) from preculture medium when subcultures of strain PD653 (GenBank accession number DQ673618) were prepared. Strain PD653-B2 was unable to transform HCB into PCP.

The catabolic ability of strain PD653-B2 was determined by inoculating the strain into mineral salts medium (MM) containing HCB, PCNB, or PCP.

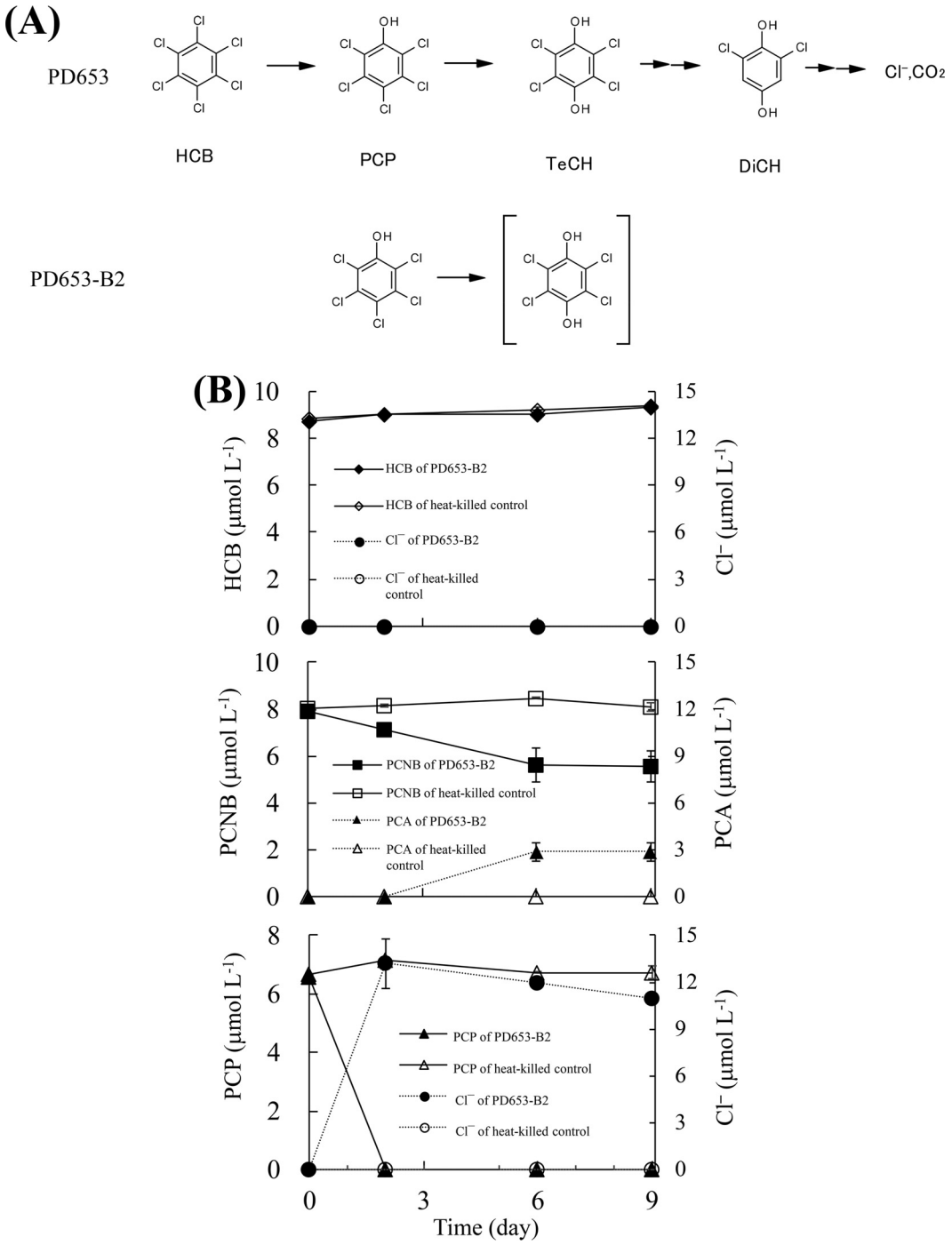

FIG 1 (A) Proposed pathway through which hexachlorobenzene and pentachlorophenol are degraded by *Nocardioides* sp. strains PD653 and PD653-B2. (B) Determination of catabolic ability of strain PD653-B2. Chloroaromatic compound degradation and Cl^- generation were analyzed. Cl^- and NO_2^- generated during the degradation of pentachloronitrobenzene (PCNB) are not shown. Each concentration shown is the mean ($n = 3$) with the standard deviation. (C) Detection and identification of PCNB-derived metabolites produced by strain PD653-B2. (Top) Authentic pentachloroaniline (PCA) standard. (Bottom) Solution of strain PD653-B2 on day 9. The UV spectrum of PCA and the metabolite indicated with an arrow are also shown. (D) Spectrum of PCA acquired by gas chromatography mass spectrometry. (Top) Authentic PCA standard. (Bottom) The unknown metabolite of pentachloronitrobenzene on day 9.

We found no HCB degradation or chloride ion accumulation. In contrast, 30.4% of the PCNB (initial concentration of 8 μmol liter^{-1}) was degraded. No liberation of nitrite or chloride ions was found (data not shown), but an unidentified peak was found when the culture solution was analyzed by high-performance liquid chromatography (HPLC)

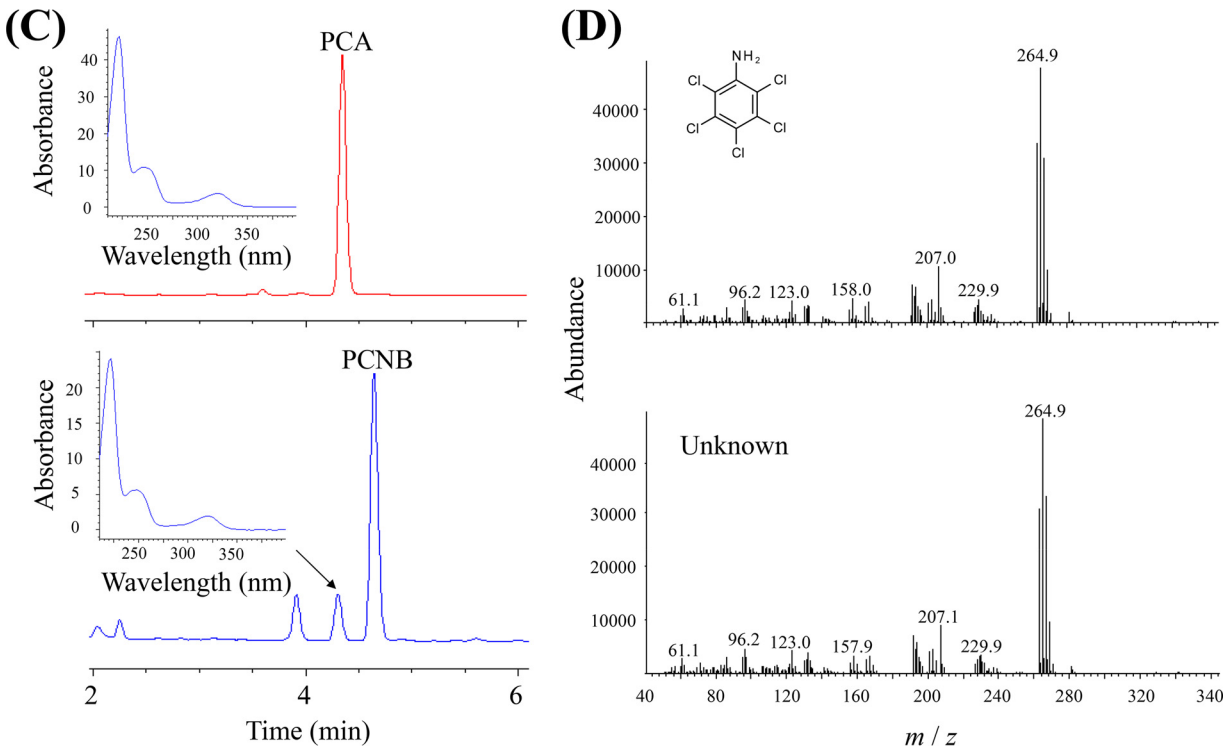

FIG 1 (Continued)

on days 6 and 9. The retention time and mass spectrum of the unidentified peak were consistent with the compound being pentachloroaniline (PCA) (Fig. 1D). All of the PCP disappeared when the PD653-B2 strain was cultivated in a solution containing PCP at a concentration of 6.4 μmol liter^{-1} for 9 days, and the chloride concentration reached 10.9 μmol liter^{-1}, suggesting approximately two chlorine atoms were released per PCP molecule through dechlorination (Fig. 1B).

Comparative genome analysis revealed a region conserved only in strain PD653. We hypothesized that the derivative strain PD653-B2 lacked the ability to degrade HCB and PCNB because of a genetic rearrangement leading to the genomic region harboring the genes coding for enzymes involved in HCB and PCNB metabolism being deleted. This hypothesis was tested by fully sequencing the native and derivative strain genomes and comparing the results to identify regions that had been deleted from the derivative strain genome.

The estimated genome sizes (assembled sequence size) of the native PD653 strain and the derivative PD653-B2 strain were 5.08 Mb (87 contigs) and 4.99 Mb (81 contigs), respectively. Both genomes had G+C contents of 70.9%. The assembled strain PD653 and PD653-B2 data were subjected to DDBJ MiGAP, and 5,087 and 4,968 coding sequences, respectively, were identified. The draft genomes were compared using the Mauve tool (20), and a region of interest from positions 1 to 71,874 of contig 22 (GenBank accession number BDJG01000022) was found in which a deletion (indicated by an asterisk in Fig. 2A) consisting of 96 coding sequences had occurred in strain PD653-B2. The raw reads of strain PD653-B2 were mapped directly to contig 22 in strain PD653 to determine whether the region of interest was completely deleted from strain PD653-B2. The raw reads were completely assembled to strain PD653 contig 22, suggesting that the region of interest may not have been deleted but remained partially present in strain PD653-B2 (data not shown). This indicated that misassembly may have occurred, so we analyzed the sequences marked "b" and "c" in Fig. 2A. This confirmed that the sequences were consistent with those obtained from MiSeq, indicating that the genome structure shown in Fig. 2A was appropriate.

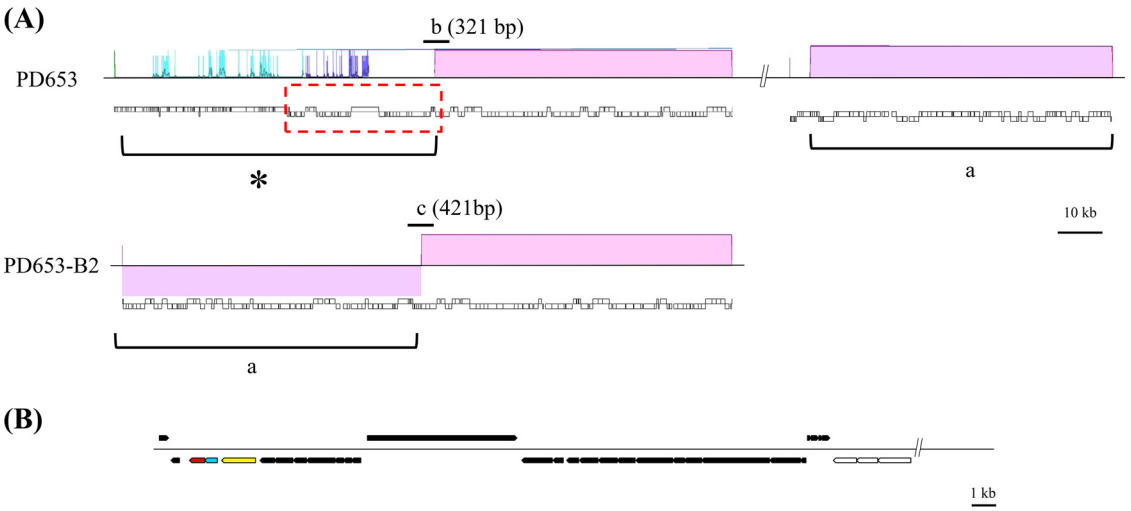

FIG 2 Comparative analysis of the *Nocardioides* sp. strain PD653 and PD653-B2 genomes. (A) The region present only in strain PD653 (lower column) is indicated with an asterisk (*). The translocated segments are marked "a." The regions amplified to confirm that misassembly had occurred are marked "b" and "c" (not to scale). (B) Structure of the locus marked with a red dotted line in panel A. The arrows indicate the sizes, locations, and directions of open reading frame (ORF) transcription. The genes located in the region marked with an asterisk (*) are marked with black arrows, and the genes conserved in both strains are marked with open arrows. The ORF1, ORF2, and ORF3 candidate genes are marked with yellow, azure, and magenta arrows, respectively.

In the region of interest, the annotations and structures indicated that the open reading frames (ORFs) ORF1, ORF2, and ORF3 were produced by the genes that most probably encode enzymes involved in the initial HCB metabolism step (Fig. 2B and Table 1). ORF1 was predicted to code coenzyme F_{420}-dependent N^5,N^{10}-methylenetetrahydromethanopterin reductase and related flavin-dependent oxidoreductases (encoded by PD653_2189). ORF2 was predicted to code a flavoprotein (encoded by PD653_2188), and ORF3 was predicted to code a conserved protein/domain typically associated with flavoprotein oxygenases in the DIM6/NTAB family (encoded by PD653_2187). Multicomponent enzyme systems are often involved in aromatic compound hydroxylation, so we assumed that ORF1, ORF2, and ORF3 belong to a multicomponent monooxygenase system and selected them as candidate genes. An approximately 60-kb segment of the strain PD653-B2 genome, assigned as contig 64 in strain PD653 (marked "a" in Fig. 2A) (GenBank accession number BDJG01000064), was translocated to the region containing the candidate genes in strain PD653, suggesting that genome rearrangement had occurred in strain PD653-B2.

Analysis of the genes presumed to be involved in the lower pathway revealed that an ORF annotated as 4-hydroxyphenylacetate 3-hydroxylase (encoded by PD653_1114 in PD653 and PD653B2_0297 in PD653-B2) was similar to TftD, chlorophenol 4-monooxygenase in *Burkholderia cepacia* strain AC1100 (590 bit; 54% identity) (21). The *tftC* gene encoding flavin reductase was not found close to this ORF, but the putative flavin reductase gene was found upstream of the ORF (PD653_1112 in PD653 and PD653B2_0299 in PD653-B2). A gene cluster containing an ORF encoding a protein homologous to 2,6-dichlorophenol hydroxylase (TfdB; 55% identify) in *Ralstonia eutropha* strain JMP 134 was found (encoded by PD653_3537 in PD653 and PD653B2_3864 in PD653-B2) (22). An ORF encoding a protein homologous to maleylacetate reductase (TfdF; 40% identity) was also found adjacent to the putative *tfdB* gene (23). The *pcp* genes responsible for PCP degradation were not found in the draft genome of either strain.

Nucleotide and amino acid sequence analyses of the *hcb* genes. A short ORF (called ORF2a) was found in the flanking region of 177 nucleotides between ORF1 and ORF2. The ORF2a termination codon overlapped with the downstream ORF2 start codon (Fig. 3A). Similarly, the ORF2 stop codon overlapped with the ORF3 start codon. The putative ribosome-binding sites GAAAGAA and GGAAAG were found 10 nucleo-

TABLE 1 List of CDSs identified in the region present only in strain PD653[a]

Locus tag	Gene length (bp)	Protein length (aa)[b]	Closest related protein	Bit score	*E*-value	Identity (%)	Accession no.	Organism
PD653_2118	483	161	RusA family crossover junction endodeoxyribonuclease	129	2.0e-35	51	WP_050670494	*Luteipulveratus halotolerans*
PD653_2119	771	257	RusA family crossover junction endodeoxyribonuclease	106	5.0e-24	38	WP_064943947	*Mycobacterium* sp. 852013-50091_SCH5140682
PD653_2120	312	104	Hypothetical protein TPY_2741	112	4.0e-29	53	AEJ40901	*Sulfobacillus acidophilus* TPY
PD653_2121	762	254	Site-specific DNA methyltransferase	325	9.0e-110	63	WP_015297969	*Mycobacterium* sp. JS623
PD653_2122	300	100	Lsr2 family protein	48.5	5.0e-05	31	WP_029146266	*Microbacterium luticocti*
PD653_2123	363	121	Hypothetical protein	63.9	4.0e-11	41	WP_028474062	*Nocardioides alkalitolerans*
PD653_2124	585	195	Adenine methyltransferase	244	9.0e-80	71	WP_074404865	*Mycobacterium fortuitum*
PD653_2125	894	298	Hypothetical protein	205	1.0e-62	66	WP_038679418	*Pimelobacter simplex*
PD653_2126	1,680	560	DnaB-like helicase N-terminal domain-containing protein	672	0.0	67	SFI85990	*Nocardioides psychrotolerans*
PD653_2127	678	226	Hypothetical protein SAMN05216561_11433	273	3.0e-90	64	SFI86065	*Nocardioides psychrotolerans*
PD653_2128	456	152	DUF4326 domain-containing protein	109	3.0e-28	47	WP_067955981	*Mycobacterium* sp. NAZ190054
PD653_2129	309	103	Protein of unknown function	100	9.0e-24	59	SDT36843	*Jiangella* sp. DSM 45060
PD653_2130	270	90	GTPase ObgE	35.4	6.1e+00	73	WP_075711905	*Eubacterium* sp. 68-3-10
PD653_2131	306	102	Hypothetical protein	120	9.0e-34	61	WP_055962014	*Aeromicrobium* sp. Leaf291
PD653_2132	204	68	Alkaline phosphatase	35	3.7e+00	50	WP_011847724	*Shewanella baltica*
PD653_2133	366	122	Hypothetical protein SAMN05216561_11438	39.3	2.1e-01	39	SFI86241	*Nocardioides psychrotolerans*
PD653_2134	294	98	Hypothetical protein	45.1	5.0e-04	35	WP_018793587	*Salinispora arenicola*
PD653_2135	273	91	Bifunctional (p)ppGpp synthetase/ guanosine-3′,5′-bis(diphosphate) 3′-pyrophosphohydrolase	38.1	6.6e-01	32	WP_059580539	*Burkholderia vietnamiensis*
PD653_2136	186	62	Hypothetical protein SAMN05216561_11439	60.8	3.0e-10	57	SFI86273	*Nocardioides psychrotolerans*
PD653_2137	201	67						
PD653_2138	201	67	Hypothetical protein TREMEDRAFT_64958	36.6	1.1e+00	43	XP_007007165	*Tremella mesenterica* DSM 1558
PD653_2139	1,455	485	Hypothetical protein SAMN05216561_11441	522	2.0e-180	57	SFI86340	*Nocardioides psychrotolerans*
PD653_2140	297	99	Hypothetical protein	66.2	3.0e-12	42	WP_038676231	*Pimelobacter simplex*
PD653_2141	156	52	3-Dehydroquinate synthase	33.1	8.4e+00	60	WP_036384679	*Muricauda* sp. MAR_2010_75
PD653_2142	1,482	494	Hypothetical protein	566	0.0	67	WP_018585440	*Salinispora arenicola*
PD653_2143	1,554	518	Hypothetical protein SAMN05216561_11447	701	0.0	70	SFI86582	*Nocardioides psychrotolerans*
PD653_2144	198	66	DUF2283 domain-containing protein	56.2	1.0e-08	54	WP_051681722	*Cellulomonas* sp. HZM
PD653_2145	717	239	HNH endonuclease	114	4.0e-28	38	WP_060921055	*Microbacterium paraoxydans*
PD653_2146	531	177	Hypothetical protein AHiyo6_03890	80.9	3.0e-15	61	GAP53824	*Arthrobacter* sp. Hiyo6
PD653_2147	306	102						
PD653_2148	189	63	Hypothetical protein F443_18763	32.7	6.4e+00	48	ETI34804	*Phytophthora parasitica* P1569
PD653_2149	201	67	Hypothetical protein	55.1	1.0e-08	42	WP_038679443	*Pimelobacter simplex*
PD653_2150	1,068	356	Phage Mu protein F-like protein	477	2.0e-166	69	SFI86619	*Nocardioides psychrotolerans*
PD653_2151	1,254	418	Hypothetical protein SAMN05216561_11449	468	9.0e-161	63	SFI86659	*Nocardioides psychrotolerans*
PD653_2152	408	136	Uncharacterized conserved protein	142	2.0e-41	59	SFI86700	*Nocardioides psychrotolerans*
PD653_2153	1,152	384	Hypothetical protein SAMN05216561_11451	619	0.0	77	SFI86736	*Nocardioides psychrotolerans*
PD653_2154	420	140						
PD653_2155	333	111	Hypothetical protein SAMN05216561_11456	105	4.0e-27	58	SFI86932	*Nocardioides psychrotolerans*
PD653_2156	435	145	Hypothetical protein SAMN05216561_11453	87.8	2.0e-19	47	SFI86816	*Nocardioides psychrotolerans*
PD653_2157	372	124	Phage protein, HK97 gp10 family	141	5.0e-41	58	SFI43596	*Nocardioides psychrotolerans*
PD653_2158	495	165	Hypothetical protein SAMN05216561_11455	159	3.0e-47	56	SFI86892	*Nocardioides psychrotolerans*
PD653_2159	231	77	Hypothetical protein	51.6	1.0e-06	49	WP_038679463	*Pimelobacter simplex*
PD653_2160	513	171	Hypothetical protein SAMN05216561_11458	233	3.0e-76	66	SFI87011	*Nocardioides psychrotolerans*
PD653_2161	636	212	Hypothetical protein SAMN05216561_11459	171	2.0e-50	47	SFI87042	*Nocardioides psychrotolerans*
PD653_2162	180	60	Hypothetical protein SAMN05216561_11460	68.6	2.0e-13	58	SFI87082	*Nocardioides psychrotolerans*
PD653_2163	3,390	1,130	Phage tail tape measure protein, TP901 family, core region	415	2.0e-122	48	SDD40725	*Auraticoccus monumenti*
PD653_2164	1,812	604	Hypothetical protein	87	2.0e-14	24	WP_038676804	*Pimelobacter simplex*
PD653_2165	1,014	338	Hypothetical protein	107	1.0e-22	29	WP_038676802	*Pimelobacter simplex*
PD653_2166	315	105						
PD653_2167	321	107						
PD653_2168	201	67						

(Continued on next page)

TABLE 1 (Continued)

Locus tag	Gene length (bp)	Protein length (aa)[b]	Closest related protein	Bit score	*E*-value	Identity (%)	Accession no.	Organism
PD653_2169	342	114						
PD653_2170	363	121	Hypothetical protein	97.4	3.0e-24	67	WP_056903920	*Nocardioides* sp. Leaf307
PD653_2171	732	244	Hypothetical protein	80.1	3.0e-14	31	WP_052337072	*Nocardioides alkalitolerans*
PD653_2172	678	226	Hypothetical protein	77.4	2.0e-13	31	WP_027768815	*Streptomyces* sp. CNQ865
PD653_2173	222	74	Hypothetical protein	78.2	1.0e-17	53	WP_026923285	*Glycomyces arizonensis*
PD653_2174	192	64	Hypothetical protein	76.3	4.0e-17	60	WP_067428397	*Nocardioides jensenii*
PD653_2175	2,709	903	Polysaccharide deacetylase	103	2.0e-19	63	ONH30622	*Frankia* sp. M16386
PD653_2176	402	134	Hypothetical protein AUJ48_03015	108	7.0e-26	46	OIN95531	*Deltaproteobacteria* bacterium CG1_02_45_11
PD653_2177	189	63	Hypothetical protein	58.5	2.0e-08	52	WP_018018316	*Corynebacterium capitovis*
PD653_2178	180	60	Multispecies: hypothetical protein	63.2	4.0e-12	50	WP_056689176	*Nocardioides*
PD653_2179	924	308	Hypothetical protein	342	1.0e-114	61	WP_041545914	*Nocardioides* sp. JS614
PD653_2180	174	58	Aryl-alcohol oxidase	35.4	1.9e+00	34	KDQ59695	*Jaapia argillacea* MUCL 33604
PD653_2181	1,068	356	DUF4192 domain-containing protein	413	2.0e-141	59	WP_056689300	*Nocardioides* sp. Root140
PD653_2182	681	227	Hypothetical protein	317	6.0e-107	70	WP_011751463	*Nocardioides* sp. JS614
PD653_2183	504	168	Hypothetical protein	129	4.0e-35	52	WP_043806996	*Paenarthrobacter aurescens*
PD653_2184	1,128	376	Hypothetical protein SAMN05428985_101622	179	2.0e-49	40	SDJ82508	*Nocardioides* sp. YR527
PD653_2185	369	123	Hypothetical protein	74.3	3.0e-15	45	WP_056689157	*Nocardioides* sp. Root140
PD653_2186	336	112	Hypothetical protein SAMN04487968_110141	35.8	7.3e+00	62	SFC74443	*Nocardioides terrae*
PD653_2187	621	207	Flavin reductase	212	4.0e-67	64	WP_071047937	*Frankia* sp. BMG5.36
PD653_2188	507	169	FMN reductase	212	5.0e-68	68	WP_029112870	*Mycobacterium* sp. URHB0044
PD653_2189	1,356	452	LLM class flavin-dependent oxidoreductase	538	0.0	58	WP_061291802	*Azotobacter vinelandii*
PD653_2190	585	195	Multispecies: thermonuclease	252	9.0e-83	70	WP_011776883	*Micrococcaceae*
PD653_2191	750	250	Hypothetical protein SAMN05216467_2870	209	1.0e-64	55	SFK31985	*Cellulomonas* sp. KH9
PD653_2192	531	177	Hypothetical protein WILDE_87	60.5	3.0e-08	39	ALY10869	*Arthrobacter* phage Wilde
PD653_2193	1,149	383	Hypothetical protein	258	3.0e-81	70	WP_011751639	*Nocardioides* sp. JS614
PD653_2194	351	117	Hypothetical protein	38.9	3.8e-01	49	WP_041545943	*Nocardioides* sp. JS614
PD653_2195	324	108	Hypothetical protein	35.4	5.7e+00	24	WP_006292151	*Parascardovia denticolens*
PD653_2196	378	126	Hypothetical protein ARZXY2_4076	142	3.0e-41	82	AOY73576	*Arthrobacter* sp. ZXY-2
PD653_2197	6,069	2,023	DNA primase	2,971	0.0e+00	76	WP_057294205	*Nocardioides* sp. Soil796
PD653_2198	1,233	411	DNA polymerase V	439	1.0e-149	59	SDL33667	*Nocardioides* sp. YR527
PD653_2199	414	138	DNA polymerase V	97.1	4.0e-23	45	KXS38722	*Halomonadaceae* bacterium T82-2
PD653_2200	483	161	Hypothetical protein	268	2.0e-90	83	WP_011751413	*Nocardioides* sp. JS614
PD653_2201	756	252	Hypothetical protein	290	3.0e-96	59	WP_057294213	*Nocardioides* sp. Soil796
PD653_2202	756	252	Chromosomal replication initiator DnaA	300	3.0e-100	67	WP_056689293	*Nocardioides* sp. Root140
PD653_2203	723	241	Hypothetical protein	363	2.0e-125	77	WP_011751416	*Nocardioides* sp. JS614
PD653_2204	1,491	497	Membrane protein	867	0.0e+00	87	WP_011776835	*Paenarthrobacter aurescens*
PD653_2205	465	155	Hypothetical protein	191	2.0e-59	63	WP_067431475	*Nocardioides jensenii*
PD653_2206	708	236	Hypothetical protein	223	2.0e-70	62	WP_056689283	*Nocardioides* sp. Root140
PD653_2207	2,739	913	Transglycosylase	1,288	0.0	72	WP_067431470	*Nocardioides jensenii*
PD653_2208	483	161	ATP-binding protein	291	1.0e-94	90	WP_067431563	*Nocardioides jensenii*
PD653_2209	822	274	Hypothetical protein	256	4.0e-81	58	WP_076180369	*Mycobacterium fortuitum*
PD653_2210	207	69						
PD653_2211	153	51	Hypothetical protein SAMN05421872_102369	44.7	6.0e-05	49	SDC47105	*Nocardioides lianchengensis*
PD653_2212	297	99	Hypothetical protein SAMN05421872_101566	58.9	3.0e-09	38	SDC21565	*Nocardioides lianchengensis*
PD653_2213	297	99	DUF3263 domain-containing protein	127	3.0e-36	70	WP_062101763	*Cellulomonas* sp. B6

[a]Coding sequences (CDSs) that exhibited no similarity to proteins in the public databases are blank.
[b]aa, amino acids.

tides upstream of ORF2 and 15 nucleotides upstream of ORF3, respectively. The GC TGGC hexamer, which was similar to the hexamer in *Streptomyces glaucescens* (24, 25), was 35 nucleotides upstream of ORF2 and 48 nucleotides upstream of ORF3, suggesting it is a promoter.

The amino acid sequence deduced for ORF1 was similar to the sequence in Ese, the monooxygenase enzyme involved in endosulfan and endosulfan sulfate metabolism, in *Arthrobacter* sp. KW (432 bits; 49% identity) (26). Ese belongs to the two-component flavin-dependent monooxygenase family. The distribution of secondary structural elements was predicted from the deduced ORF1 amino acid sequence, and it was similar to other known flavin-dependent monooxygenases with conformations that have been

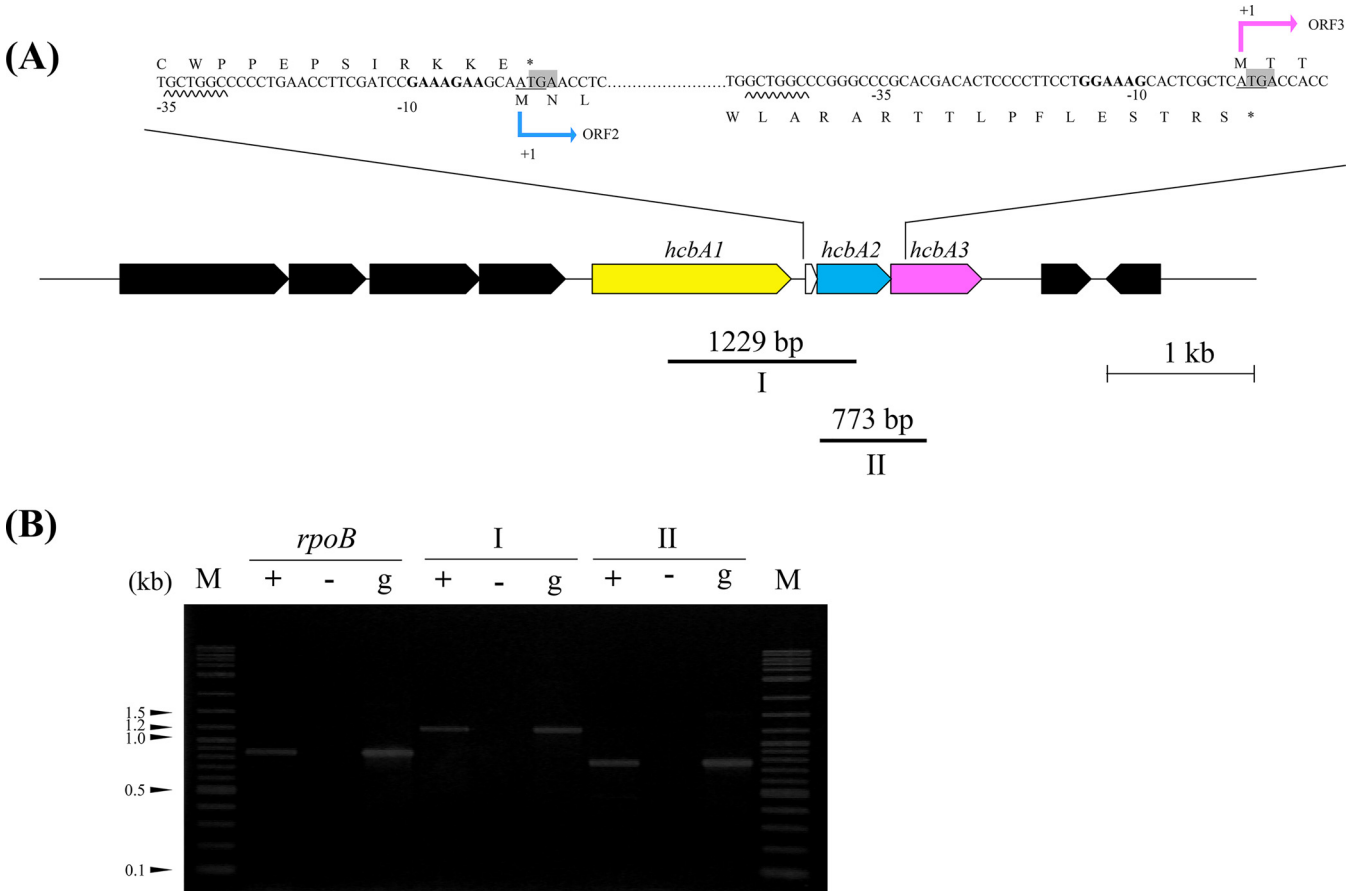

FIG 3 (A) Schematic representation of the candidate gene flanking region for *Nocardioides* sp. strain PD653 with putative ribosome-binding sites. The initiation codons (ATG or GTG) are underlined. The termination codons (TGA) are shaded. The translation start sites (+1) are shown. The putative promoter regions are underlined with wavy lines. The putative ribosome-binding sites are marked with bold letters. The candidate genes ORF1, ORF2, ORF3, and small ORF2a are marked with yellow (*hcbA1*), azure (*hcbA2*), magenta (*hcbA3*), and open arrows, respectively. The regions amplified for reverse transcription-PCR (RT-PCR) analysis are indicated below. The primer binding site and target amplified region of *rpoB* are not shown. (B) Polycistronic transcription of *hcbA* genes. Intergenic regions I and II were analyzed by RT-PCR. No-RT and genomic DNA, used as negative and positive controls, respectively, are presented in lanes − and +, respectively. cDNA from strain PD653 cells exposed to hexachlorobenzene for 3 h was used as the template.

determined (Fig. 4). The deduced ORF2 amino acid sequence was similar to the sequence in EmoB, an NADH:flavin mononucleotide oxidoreductase in *Mesorhizobium* sp. BNC1 involved in the two-component enzyme system (77 bits; 37% identity) (27). The deduced ORF3 amino acid sequence contained a flavin reductase-like domain (smart00903). The secondary structure of ORF3 was predicted in a similar way to the secondary structure of ORF1 and had a strongly conserved distribution of known flavin reductase secondary structural elements except for strand $\beta 4$ (see Fig. S1 in the supplemental material).

Degradation of HCB and PCNB by recombinant *E. coli* cells. We determined whether the products of ORF1, ORF2, and ORF3 contributed to HCB and PCNB degradation by determining the abilities of recombinant *E. coli* BL21(DE3) cells harboring each construct to degrade HCB when incubated for 12 h in a medium containing HCB at 10 μmol liter^{-1} (Fig. 5A, solid bars). The degradation activities of *E. coli* cells containing plasmids separately carrying ORF1, ORF2, and ORF3 were first compared. *E. coli* BL21(DE3)/pE1N (ORF1 at the first multicloning site [MCS1]) degraded 3.9% of the HCB, and *E. coli* cells harboring pE2N (ORF2 at MCS1) or pE3N (ORF3 at MCS1) did not degrade HCB at all. The HCB-degrading activities of the two ORFs in the coexpression system were then compared. *E. coli* BL21(DE3)/pE13N2 (ORF1 at MCS1 and ORF3 at the second multicloning site [MCS2]) degraded 68.7% of the HCB, but *E. coli* BL21(DE3)/pE12N2 (ORF1 at MCS1 and ORF2 at MCS2), pE12N (ORF1 and ORF2 at MCS1), and

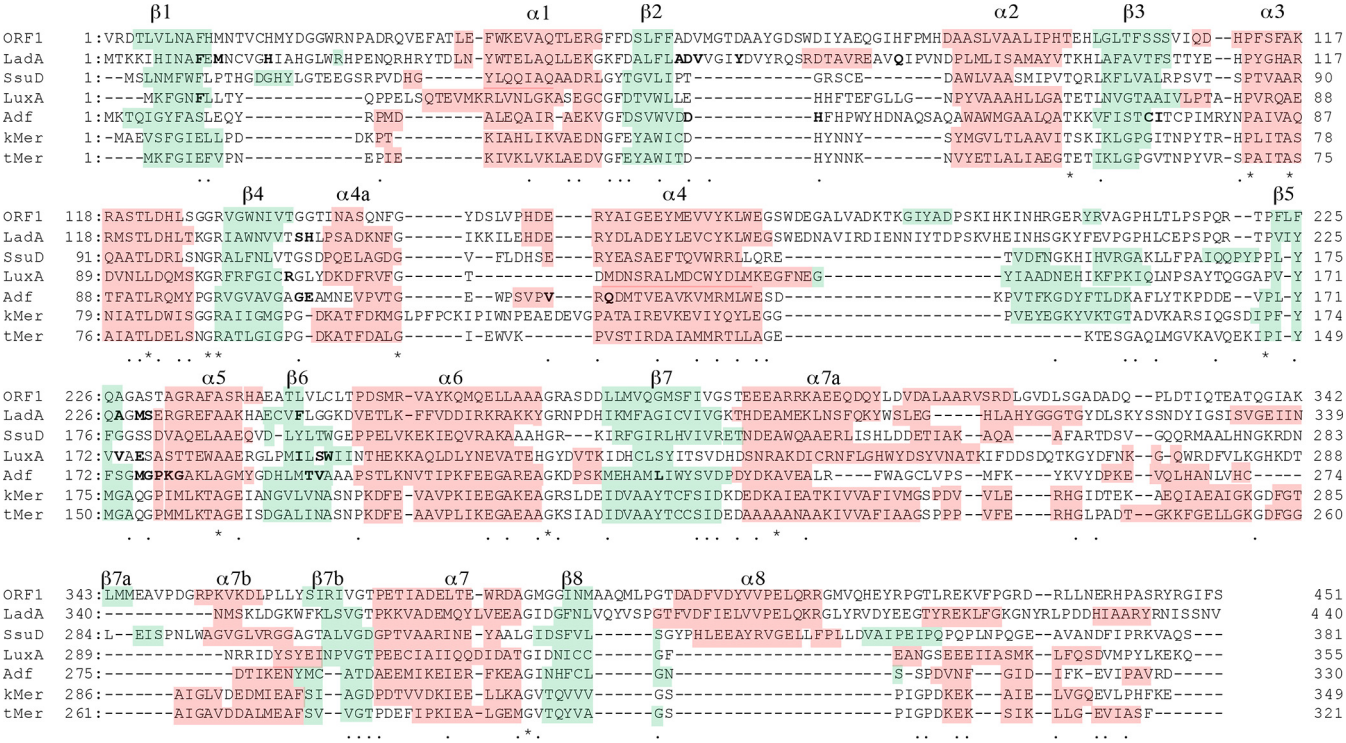

FIG 4 Comparison of the deduced amino acid sequences of ORF1 and other flavin-dependent monooxygenases. Secondary structural elements are highlighted in green for β-sheets and red for α-helices. ORF1, hexachlorobenzene oxidative dehalogenase from *Nocardioides* sp. PD653; LadA, long-chain alkane monooxygenase from *Geobacillus thermodenitrificans* NG80-2 (gi 165761309) (32, 33); SsuD, alkanesulfonate monooxygenase from *Escherichia coli* (gi 2507139) (34); LuxA, alkanal monooxygenase from *Vibrio harveyi* (gi 126509) (35); Adf, F_{420}-dependent secondary alcohol dehydrogenase from *Methanobacterium thermophilus* (gi 47168785) (36); kMer, coenzyme F_{420}-dependent methylenetetrahydromethanopterin reductase from *Methanobacterium kandleri* (gi 126509) (37); tMer, coenzyme F_{420}-dependent methylenetetrahydromethanopterin reductase from *Methanobacterium thermoautotrophicum* (gi 13787050) (37). Identical residues are marked with asterisks, and conserved residues are marked with dots. Residues involved in coenzyme binding are labeled with bold letters.

pE23N2 (ORF2 at MCS1 and ORF3 at MCS2) did not degrade HCB. HCB was degraded most effectively (83.0%) by *E. coli* BL21(DE3)/pE123N (ORF1 and ORF2 at MCS1 and ORF3 at MCS2), which coexpressed all three ORFs. An unknown peak that indicated HCB degradation activity was found when the *E. coli* BL21(DE3)/pE123N culture fluid was analyzed by HPLC (Fig. 5B). The peak had the same retention time as PCP (data not shown) and was identified as PCP because the mass spectrum was identical to the mass spectrum of the PCP standard (Fig. 5C). As HCB was degraded, PCP was stoichiometrically accumulated (Fig. 5D), suggesting that HCB was dehalogenated to give PCP as shown in Fig. 5A (open bars). Recombinant *E. coli* cells harboring pE123N at a dry weight cell concentration of 0.8 g liter^{-1} degraded 6.9 μmol liter^{-1} HCB within 6 h, giving a degradation rate of 1.44 nmol mg^{-1} h^{-1} on a dry cell weight basis.

The dechlorination of HCB was strongly affected by the presence of oxygen (Fig. 5E). HCB was not degraded and PCP was not generated under oxygen-limited conditions, but HCB degradation and PCP generation resumed when oxygen was reintroduced by replacing the N_2 atmosphere with ambient air. When the oxygen concentration was increased, 4 μmol liter^{-1} HCB was transformed into PCP in 3 h, suggesting that ORF1 encodes a monooxygenase. We hypothesized that ORF1, ORF2, and ORF3 are genes that are involved in the initial HCB dechlorination step, so we called them *hcbA1*, *hcbA2*, and *hcbA3*, respectively.

We determined whether the *hcbA* genes are involved in PCNB degradation by investigating the PCNB degradation and metabolite generation time courses using *E. coli* BL21(DE3)/pE123N. As shown in Fig. 5D, the recombinant cells degraded 8 μmol liter^{-1} PCNB within 6 h. PCP was found to be a metabolite and was accumulated stoichiometrically.

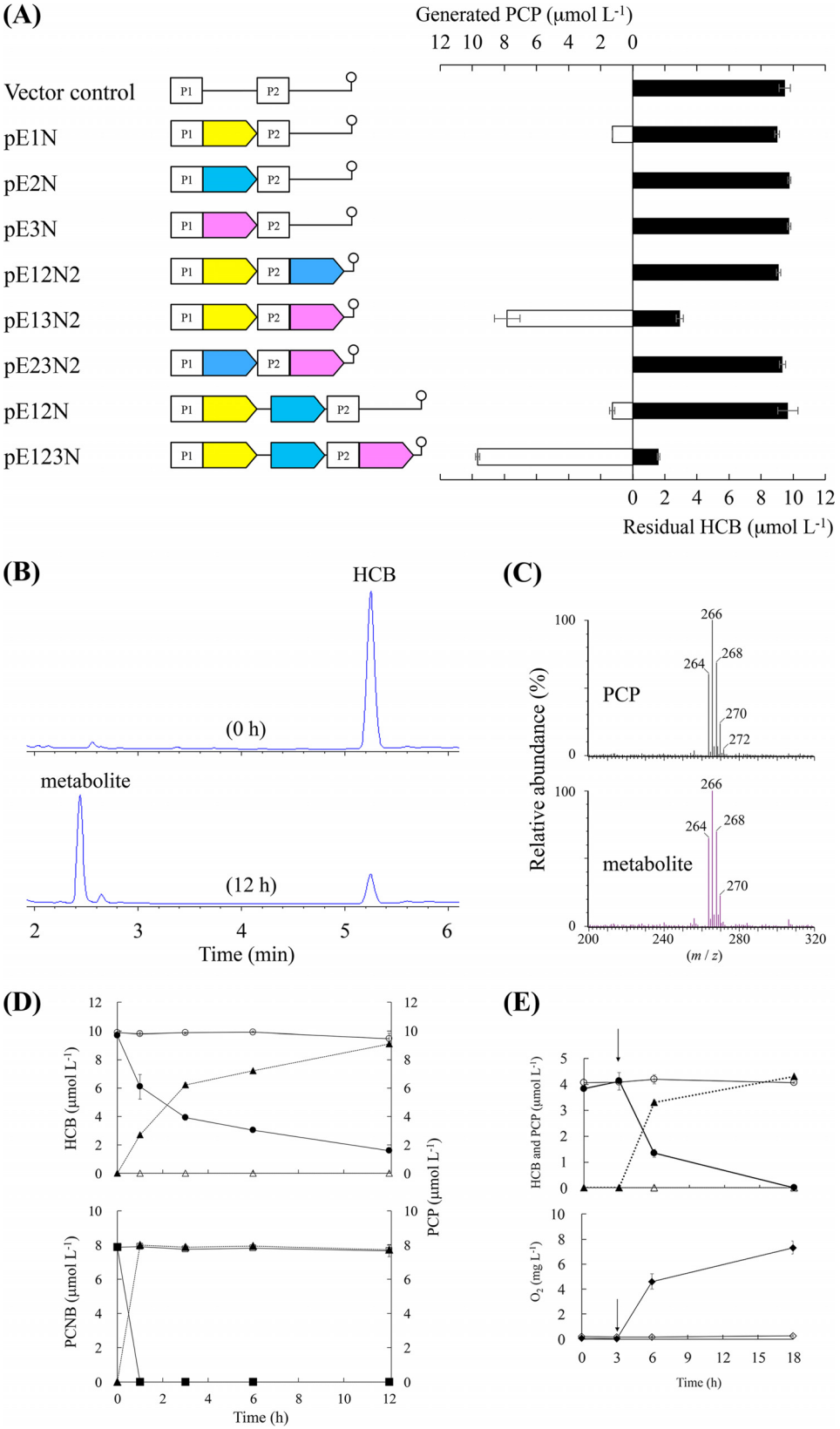

FIG 5 Transformation of hexachlorobenzene (HCB) by recombinant *Escherichia coli* cells. (A) Comparison of dechlorination activity for *E. coli* cells transformed using expression vectors. Solid and open bars indicate residual HCB and pentachlorophenol (PCP) generated in the culture, respectively. Each error bar indicates the standard error for triplicate samples. The genetic elements of all of the expression vectors are shown; the candidate genes

(Continued on next page)

Operon structures of *hcbA1*, *hcbA2*, and *hcbA3*. We determined whether the three identified genes were transcribed polycistronically by analyzing the intergenic regions *hcbA1-hcbA2* (region I) and *hcbA2-hcbA3* (region II) by reverse transcription-PCR (RT-PCR) using as a template total RNA extracted from strain PD653 cells grown in a medium containing HCB. Both intergenic regions were successfully amplified, suggesting that all three genes were transcribed as a single mRNA molecule (Fig. 3B).

DISCUSSION

The PD653-B2 and PD653 strains had different abilities to dechlorinate HCB and denitrate PCNB (28). Interestingly, an approximately equal molar amount of PCA was generated when PCNB was degraded by PD653-B2, so we hypothesized that there was an alternative degradation pathway. The results suggest that the gene(s) involved in both HCB dechlorination and PCNB denitration was deleted when PD653-B2 was derived from PD653. Comparative genome analysis indicated that the approximately 60-kb region marked with an asterisk in Fig. 2A was present in PD653 but not in PD653-B2. Direct read mapping results led us to suspect that misassembly may have occurred in this region, but the sequence accuracy obtained from MiSeq was supported by PCR amplification and sequence analysis. As a result, the region of interest (marked with an asterisk in Fig. 2A) may have been translocated and less likely to be sequenced by MiSeq because of mutations in strain PD653-B2.

In the region of interest, almost half of the coding sequence (42/96) had similar sequences to genes in the *Nocardioides* genus (Table 1), suggesting that the region is not unique to strain PD653. Efforts were made to search the 60-kb region for inverted repeat sequences recognized by transposase and for genes encoding transposase typical of insertion sequence elements known to be involved in genetic rearrangements (29), but none were detected (data not shown). There were, therefore, no clues to allow us to gain an understanding of how the genomic rearrangement occurred. Comparative genome analysis did not allow us to identify *hcbA* genes in the chromosome or plasmid of the native PD653 strain.

Recombinant *E. coli* cells biotransformed HCB and PCNB into PCP. It was found in a previous study that genetically engineered *Sphingobium chlorophenolicum* ATCC 32723 harboring a gene cassette (*camA*$^+$ *camB*$^+$ *camC*) degraded HCB at a rate of 0.67 nmol mg^{-1} h^{-1} on a dry cell weight basis (11). In our assays, *E. coli* BL21(DE3)/pE123N (*hcbA1* and *hcbA2* at ORF1 and *hcbA3* at ORF2) degraded HCB at more than twice that rate. The deduced amino acid sequence comparisons revealed that HcbA1, HcbA2, and HcbA3 showed no significant homology to the proteins encoded by the gene cassette (*camA*$^+$ *camB*$^+$ *camC*) (9). Considering that *hcbA* genes were deleted from PD653-B2, we concluded that these genes may play important roles in the initial steps of the metabolism of both HCB and PCNB. However, it is not clear if only these genes are responsible for HCB and PCNB metabolism by PD653, so further studies of *hcbA* genes using knockout and complementation techniques are necessary.

The *hcbA* gene, which has characteristics associated with flavoproteins, was identified in *Nocardioides* sp. strain PD653. Flavoproteins are involved in various biological

FIG 5 Legend (Continued)
ORF1, ORF2, and ORF3 are marked with yellow, azure, and magenta arrows, respectively. The stem-loop symbol indicates the position of the terminator. P1 and P2 denote T7 promoters 1 and 2, respectively. The scheme is not to scale. (B) High-performance liquid chromatography chromatograms for sample solutions at 0 and 12 h. (C) PCP mass spectrum. (Top) Authentic PCP standard. (Bottom) The metabolite of HCB. (D) Time courses for HCB degradation (■) and PCP generation (▲). The HCB concentrations (□) and PCP concentrations (△) in the vector control cultures are also shown. Each concentration shown is the mean (n = 3) with the standard deviation. (D) Time courses for HCB degradation (●), pentachloronitrobenzene (PCNB) degradation (■), and PCP generation (▲). The HCB concentrations (○), PCNB concentrations (□), and PCP concentrations (△) in the vector control cultures are also shown. Each concentration shown is the mean (n = 3) with the standard deviation. (E) Effect of oxygen on HCB dechlorination by recombinant *E. coli* cells. (Top) HCB degradation (○) and PCP generation (△) under oxygen-limited conditions. The HCB concentrations (●) and PCP concentrations (▲) were determined in the replicate samples in which the N_2 atmosphere had been replaced with ambient air at the times indicated by arrows. Closed diamonds indicate the oxygen concentrations in the replicate samples to which oxygen had been reintroduced, and the open diamonds indicate the oxygen concentrations in the controls.

processes, such as the degradation of natural and anthropogenic compounds and the biosynthesis of hormones, vitamins, and antibiotics (30). Our results suggest the possibility that *hcbA1* encodes a monooxygenase responsible for transforming both HCB and PCNB into PCP. This was supported by the results obtained under oxygen-limited conditions (Fig. 5E). We propose, according to Huijbersa et al. (31), to classify HcbA1 as part of the group C flavin monooxygenases because it contains a conserved luciferase-like domain (IPR011251). This domain is found in different bacterial luciferase family proteins, including LadA produced by *Geobacillus thermodenitrificans* MG80-2 (32, 33), SsuD produced by *E. coli* (34), LuxA produced by *Vibrio harveyi* (35), and Adf (36), kMer, and tMer produced by methanogenic archaea (37), and consists of eight α-helices and eight parallel β-strands, forming a characteristic three-dimensional structure called the TIM barrel fold. Despite the low overall sequence identity, there are structural similarities between bacterial luciferases and nonfluorescent flavoproteins, which make up clearly related families with somewhat different folds (32–38). The predicted HcbA1 secondary structure was similar to the secondary structures of TIM barrel enzymes, suggesting that they have similar three-dimensional structures (Fig. 4).

The *hcbA3* gene encodes a putative reductase component associated with HcbA1. We identified a conserved domain typical of the flavin reductase component belonging to the two-component flavin-diffusible monooxygenase (TC-FDM) family, including TftC (39), PheA2 (40), and HpaC (41), from the deduced HcbA3 amino acid sequence. These enzymes catalyze the NAD(P)H-dependent reduction of flavins and supply reduced flavins to a monooxygenase (21, 39–43). Taking the comparison of secondary structural elements into account, we hypothesized that HcbA3 can fold in a similar way to TC-FDM and acts as a flavin reductase. This hypothesis was supported by the HCB degradation activity being higher when *hcbA1* and *hcbA3* were coexpressed by recombinant *E. coli* than when only *hcbA1* was expressed by recombinant *E. coli*. Therefore, the *hcbA1* and *hcbA3* genes in PD653 may encode a flavin-dependent two-component oxygenase that catalyzes the dehalogenation of HCB to PCP.

The *hcbA3* and *hcbA2* genes, which slightly overlap (by three nucleotides) (Fig. 3A) upstream of *hcbA3*, were indicative of translational coupling (44–47). Genetic organizations resembling this structure have been found in several Gram-positive bacterial gene clusters involved in the degradation of long-chain *n*-alkanes (48), thiocarbamate (49), vinyl chloride, and ethene (50). We could not fully determine the functional role of *hcbA2*, but we did find that it is part of the *hcb* operon and is transcribed polycistronically; therefore we hypothesized that it is part of the three-component enzyme system that catalyzes the oxidative dehalogenation of HCB in strain PD653 cells. Further studies of protein-protein interactions and the biochemical properties of the *hcb* gene products should be performed to test this hypothesis.

In conclusion, we describe the characterization of the *hcb* operon in *Nocardioides* sp. strain PD653 that transforms HCB and PCNB into PCP under aerobic conditions. This strain has previously been found to completely mineralize HCB under aerobic conditions (13). We did not identify genes similar to known PCP-degrading genes in the draft PD653 genome, but ongoing work is aimed at locating genes that may encode PCP-degrading enzymes.

MATERIALS AND METHODS

Materials. PCA was purchased from TCI Tokyo Casei (Tokyo, Japan). PCNB and PCP were purchased from Wako Pure Chemical Industries (Osaka, Japan). HCB was purchased from Dr. Ehrenstorfer GmbH (Augsburg, Germany). Difco R2A agar medium was purchased from Becton Dickinson and Company (Franklin Lakes, NJ, USA). MM was prepared as previously described (51) and then autoclaved and supplemented with 50 μg liter^{-1} *p*-aminobenzoic acid. The preculture medium for strains PD653 and PD653-B2 contained 1 g glucose, 1 g Bacto tryptone, 0.3 g $(NH_4)_2SO_4$, 1.2 g $Na_2HPO_4{\cdot}12H_2O$, and 0.5 g liter^{-1} KH_2PO_4. The preculture medium was autoclaved and then supplemented with 10 ml of a solution of trace elements (52) and 50 μg liter^{-1} *p*-aminobenzoic acid.

Analytical methods. Chloride ion concentrations were measured by ion chromatography (761 Compact IC; Metrohm, Herisau, Switzerland). An IC SI-90 4E column (Shodex, Tokyo, Japan) was used, and the mobile phase, 1.8 mM Na_2CO_3 and 1.7 mM $NaHCO_3$, was used at a flow rate of 1.0 ml min^{-1} at 40°C. The concentrations of all of the chloroaromatic compounds were monitored by HPLC (Hewlett-Packard series 1100; Hewlett-Packard, Waldbronn, Germany) equipped with a UV detector (set at 220 nm). A

TABLE 2 Bacterial strains and plasmids used in the study

Strain or plasmid	Relevant characteristics[a]	Reference or origin
Strain		
Nocardioides sp. PD653	HCB^+, PCP^+	13
Nocardioides sp. PD653-B2	HCB^-, PCP^+	This study
E. coli DH5α	F^-, I^-, f80d*lacZ*ΔM15, Δ(*lacZ*YA-*argF*)*U169*, *deoR*, *recA1*, *endA1*, *hsdR17*(r_K^-, m_K^+), *pho A*, *supE44*, *thi-1*, *gyrA96*, *relA1*	Toyobo
E. coli BL21(DE3)	F^- *ompT* $hsdS_B$(r_B^- m_B^-) *gal dcm* λ(DE3); T7 RNA polymerase gene under the control of the *lacUV* promoter	Novagen
Plasmid		
pGEM-T Easy	Ap^r *lacZ*, pMB1-derived replicon, TA cloning vector	Promega
pGEM-T Easy::2177-2179	Ap^r, pGEM-T Easy with 2.9-kb PCR-amplified DNA fragment containing ORF1, ORF2, and ORF3 of PD653	This study
pETDuet-1	Ap^r pBR322-derived ColE1 replication, T7 promoter, two MCS, expression vector	Novagen
pE123N	Ap^r, pE12N with 0.7-kb PCR-amplified DNA fragment containing ORF3 in MCS2	This study
pE12N	Ap^r, pETDuet-1with PCR-amplified DNA fragment containing ORF1 and ORF2 in MCS1	This study
pE12N2	Ap^r, pE1N with PCR-amplified DNA fragment containing ORF2 in MCS2	This study
pE23N2	Ap^r, pE2N with PCR-amplified DNA fragment containing ORF3 in MCS2	This study
pE13N2	Ap^r, pE1N with PCR-amplified DNA fragment of ORF3 in MCS2	This study
pE1N	Ap^r, pETDuet-1 with PCR-amplified DNA fragment of ORF1 in MCS1	This study
pE2N	Ap^r, pETDuet-1 with PCR-amplified DNA fragment of ORF2 in MCS1	This study
pE3N	Ap^r, pETDuet-1 with PCR-amplified DNA fragment of ORF3 in MCS1	This study

[a]HCB^+, able to degrade hexachlorobenzene (HCB); HCB^-, unable to degrade HCB; PCP^+, able to degrade pentachlorophenol (PCP); PCP^-, unable to degrade PCP; Ap^r, ampicillin resistant.

Poroshell 120 EC-C_{18} column (150 mm long, 4.6-mm inner diameter; Agilent Technologies, Tokyo, Japan) was used, and the temperature was 40°C. The mobile phase was a mixture of acetonitrile and 0.1% phosphoric acid in water, and the pump was set to run in isocratic mode with a flow rate of 1.0 ml min^{-1}. The mobile-phase composition was 90:10 acetonitrile/aqueous phosphoric acid for HCB analysis and 87:13 acetonitrile/aqueous phosphoric acid for PCNB, PCP, and PCA analysis. PCP was analyzed using an Acquity ultraperformance liquid chromatography (UPLC) system (Waters, Milford, MA, USA) equipped with a Micromass Quattro micro API tandem quadrupole system (Waters). Mass spectra of the compounds were acquired using a Z-spray source in electrospray ionization mode and total ion current mode. The electrospray ionization conditions used to analyze PCP were a capillary voltage of 1.2 kV, a cone voltage of 17.46 V, a source temperature of 100°C, a desolvation temperature of 350°C, a cone gas flow rate of 50 liters h^{-1}, and a desolvation gas flow rate of 600 liters h^{-1}. PCP was detected in negative ion mode using an *m/z* range of 150 to 300. The ultraperformance liquid chromatography and electrospray ionization mass spectrometry systems were controlled using MassLynx 4.1 software (Waters). Separation was performed using an Acquity UPLC BEH C_{18} column (1.7-mm particle size, 2.1-mm inner diameter, 100 mm long; Waters) at 40°C. Linear gradient elution was used, using two solvents. Solvent A was 0.1% (vol/vol) acetic acid in water, and solvent B was 0.1% (vol/vol) acetic acid in acetonitrile. The flow rate was 200 μl min^{-1}, and the gradient profile was 10% solvent B for 2 min, linear change to 90% solvent B over 12 min, and 90% solvent B for 4 min. The identity of PCA was confirmed by analyzing samples using an HP6890 series gas chromatograph coupled to an HP 5973 mass selective detector. The gas chromatograph was fitted with an HT8-PCB capillary column (60 m long, 0.25-mm inner diameter; Kanto Kagaku, Tokyo, Japan). The oven temperature program started at 120°C, increased to 210°C at 20°C min^{-1}, increased to 290°C at 10°C min^{-1}, and then increased to 320°C at 25°C min^{-1}. The inlet temperature was 250°C.

Bacterial strains and plasmids. The bacterial strains and plasmids used in this study are listed in Table 2. Strain PD653-B2 (GenBank accession number LC196157) was isolated unexpectedly from the preculture medium during the subculturing of strain PD653 (GenBank accession number DQ673618), and it was found to lack the ability to transform HCB into PCP. *E. coli* cells were grown in Luria-Bertani (LB) medium. *E. coli* DH5α (Toyobo, Osaka, Japan) and BL21(DE3) (Novagen, Madison, WI, USA) were used as host strains for the plasmids pGEM-T Easy (Promega, Madison, WI, USA), pETDuet-1 (Novagen), and their derivatives. The transformants harboring the plasmids were cultured in LB medium supplemented with 100 μg ml^{-1} ampicillin.

DNA isolation. Total DNA from strains PD653 and PD653-B2 grown on R2A medium at 30°C was purified using a DNeasy Tissue kit (Qiagen, Valencia, CA, USA). Plasmid DNA from *E. coli* transformants was extracted using a Wizard miniprep system (Promega).

Characterization of strain PD653-B2. The catabolic abilities of strain PD653-B2 were determined by performing biodegradation tests. Strain PD653-B2 cells were grown in a preculture medium until the optical density at 600 nm (OD_{600}) reached ~1.2. Cells were harvested at 3,000 × *g* at 4°C for 10 min, and then the cell pellets were washed with MM and then resuspended in MM. A 1-ml aliquot of the cell suspension (OD = 1.0) was added to each of a series of 50-ml glass-stoppered Erlenmeyer flasks, each containing 9 ml of MM supplemented with one of the chloroaromatic compounds tested. The initial PCP, HCB, and PCNB concentrations were 6.5, 9, and 8 μmol $liter^{-1}$, respectively. The flasks were shaken at 180

TABLE 3 PCR primers used in the study

Primer	5′ to 3′[a]
Specific primer used for amplification of candidate genes involved in dechlorination of HCB	
orf1_F	TCAGGACAACACCGACGTCT
orf3_R	ACCTCCTGTGGTGGAGCGGA
orf1-NcoI_mcs1_F	AAACCATGGGGCGGGATACCCTTGTACTC
orf1-NcoI_mcs1_R	AAACCATGGTCAGGAGAAGATGCCCCG
orf2-NcoI_mcs1_F	AAACCATGGGGAACCTCGTCACCGTCATC
orf2-NcoI_mcs1_R	AAACCATGGTCATGAGCGAGTGCTTTCCAG
orf2-NdeI_mcs2_F	AAACATATGAACCTCGTCACCGTCATCGGC
orf2_mcs2_R	GTCATGAGCGAGTGCTTT
orf3-BspHI_mcs1_F	AAATCATGACCACCTCCGCACCGATC
orf3-BspHI_mcs1_R	AAATCATGATCAGGCGGTGGTGAGGCG
orf3-NdeI_mcs2_F	AAACATATGACCACCTCCGCACCGATC
RT-PCR primer	
hcbA1_q_F	ACCCATCGAAGATCCACAAG
hcbA2_q_ F	TGAACCTCGTCACCGTCATC
hcbA2_q_R	AACTGGTCGAGGAAGAGCTTG
hcbA3_q_R	TCAAGGGAGACTGAGGTAAAGG
rpoB_q_F	AGATCTCCGAACCACTCGAA
rpoB_q_R	TGTTGATCTTGTAGCGACCG
Primer used for amplification to confirm misassembly	
wt_MS22_F	CGCTACTACCAGGTCCTCAA
delta_MS26_F	TACTTCACCTGGTTGAGGGC
wt_delta_MS_R	AGGAGGTCTTCATGATGGTG

[a]Specified restriction sites are underlined.

rpm at 30°C for 9 days. Triplicate flasks were withdrawn at selected time points, and a 600-μl aliquot of the fluid in each flask was analyzed by ion chromatography. The remaining fluid was mixed with 18.8 ml of acetonitrile, and the mixture was centrifuged at 19,000 $\times$ *g* for 10 min. The chloroaromatic compound concentrations in the supernatant were determined by HPLC with a photodiode array detector. The metabolite of PCNB that was produced was identified by gas chromatography mass spectrometry.

Draft genome sequences and analysis. Samples of genomic DNA from strains PD653 and PD653-B2 were fragmented to approximately 500 bp using a Covaris S2-A system (Covaris, Woburn, MA, USA). A library for sequencing was prepared using a NEBNext DNA library prep master mix set for the Illumina platform (New England BioLabs, Ipswich, MA, USA), and the library samples were paired-end sequenced (2 $\times$ 300 bp) using a MiSeq sequencer and a MiSeq version 3 reagent kit (Illumina KK, Tokyo, Japan). The total read bases for strains PD653 and PD653-B2 were 2.51 and 1.90 Gb, respectively. Raw reads were trimmed and assembled *de novo* using CLC Genomics Workbench version 7.5.1 (Qiagen). The trimming parameters were as follows: ambiguous limit, 2; quality limit, 0.001; 10 5′-terminal nucleotides; and 40 3′-terminal nucleotides. The *de novo* assembly parameters were as follows: update contigs, yes; bubble size, 600; minimum contig length, 1,000; automatic word size, 51; perform scaffolding, yes; auto-detect paired distances, yes; mismatch cost, 2; insertion cost, 3; deletion cost, 3; length fraction, 0.5; and similarity fraction, 0.8. The assembled contigs of strains PD653 and PD653-B2 were annotated using the DDBJ Microbial Genome Annotation Pipeline (http://www.migap.org/index.php/en) and edited manually for entry into nucleotide sequence databases (DDBJ/ENBL/GenBank).

No complete genome was available for the reference sequence with the strain PD653 draft genome, so the distances between the contigs and the arrangement order were not clear. The strain PD653 scaffold was therefore built using a rule of filling gaps with 100 Ns between contigs, as described on the NCBI website (https://www.ncbi.nlm.nih.gov/assembly/agp/AGP_Specification/). Comparative genome analysis was performed by merging and orienting the strain PD653-B2 contigs using ABACAS (53) guided by the strain PD653 genome sequence as the reference genome. The genes involved in HCB metabolism were identified by aligning the draft strain PD653-B2 genome with the draft strain PD653 genome using Mauve (20). Strain PD653-specific sequences were identified from the aligned sequences. The candidate genes were selected according to their protein-coding sequence annotations.

The sequences in the regions indicated in Fig. 2A were analyzed to determine whether misassembly had occurred in strain PD653 contig 22 and strain PD653-B2 contig 26. The nucleotide sequences of the primers used in this experiment are shown in Table 3. Region b was amplified by PCR using primer set wt_MS22_F and wt_delta_MS_R. Region c was amplified by PCR using primer set delta_MS26_F and wt_delta_MS_R. The PCR amplicons were cloned into the pGEM-T Easy vector (Promega) and sequenced.

The putative genes involved in the lower chloroaromatic compound pathway were analyzed according to the University of Minnesota Biocatalysis/Biodegradation Database (http://eawag-bbd.ethz.ch/pcp/pcp_map.html) (54).

Comparison of the deduced amino acid sequences in the genes. The amino acid sequences that were identified were compared with the amino acid sequences of other bacterial genes using the BLAST

algorithm (https://blast.ncbi.nlm.nih.gov/Blast.cgi). Amino acid sequence alignment analysis was performed using the ClustalW program on the DDBJ website (http://clustalw.ddbj.nig.ac.jp/index.php?lang=ja). The secondary structures of HcbA1 and HcbA3 were predicted using Jpred4 (http://www.compbio.dundee.ac.uk/jpred/) (55).

Construction of expression plasmids. Primers were synthesized to amplify the candidate gene ORFs (Table 3). The region including ORF1, ORF2, and ORF3 was PCR amplified from strain PD653 genomic DNA using the primer set orf1_F and orf3_R. The PCR product was ligated into the pGEM-T Easy vector and then used as a PCR template in the experiments described below. An expression vector for putative HCB-oxidative dehalogenase was constructed by amplifying ORF1 by PCR using primer set orf1-NcoI_mcs1_F and orf1-NcoI_mcs1_R. A PCR-amplified fragment containing ORF1 was digested and ligated into the NcoI site in the first multicloning site (MCS1) of pETDuet-1, and the resulting plasmid was designated pE1N. The pE2N plasmid, including ORF2, was constructed in a similar manner using primers orf2-NcoI_mcs1_F and orf2-NcoI_mcs1_R. Plasmid pE3N was formed by amplifying the fragment containing ORF3 by PCR using primer set orf3-BspHI_mcs1_F and orf3-BspHI_mcs1_R. The PCR-amplified fragment containing ORF3 was digested with BspHI and ligated into the NcoI site of pETDuet-1. Plasmid pE12N was formed by amplifying the fragment containing ORF1 and ORF2 by PCR using primers orf1-NcoI_mcs1_F and orf2-NcoI_mcs1_R. The PCR-amplified fragment containing ORF1 and ORF2 was digested and ligated into the NcoI site of pETDuet-1. Plasmid pE12N2, containing ORF1 at MCS1 and ORF2 at the second multicloning site (MCS2) of pETDuet-1, was formed by amplifying ORF2 by PCR using primers orf2-NdeI_mcs2_F and orf2_mcs2_R. The PCR-amplified fragment containing ORF2 was digested with NdeI and cloned into the NdeI-EcoRV site (MCS2) of pE1N. Plasmids pE123N (containing ORF1 and ORF2 at MCS1 and ORF3 at MCS2), pE13N2 (containing ORF1 at MCS1 and ORF3 at MCS2), and pE23N2 (containing ORF2 at MCS1 and ORF3 at MCS2) were formed by amplifying ORF3 by PCR using primers orf3-NdeI_mcs2_F and orf3_R and then digesting and ligating the fragment into the NdeI-EcoRV sites of pE12N, pE1N, and pE2N, respectively. The recombinant plasmids were sequenced and transferred into *E. coli* BL21(DE3). *E. coli* cells harboring the expression vectors were inoculated into LB medium containing 100 μg ml^{-1} ampicillin and shaken overnight at 210 rpm and 37°C. The overnight culture was inoculated into fresh LB medium containing 100 μg ml^{-1} ampicillin and 0.25 mM isopropyl-β-thiogalactoside. The initial OD_{600} was adjusted to 0.6, and gene expression was induced in a culture kept at 37°C and shaken at 210 rpm for 4 h. The induced cells were then harvested by centrifuging the mixture at 1,800 $\times$ *g* for 10 min and washed with phosphate-buffered saline.

Degradation of HCB and PCNB by the recombinant *E. coli* cells. Washed recombinant *E. coli* cells were suspended in 1 ml of MM and inoculated into 9 ml of MM containing 10 μmol liter^{-1} HCB or 8 μmol liter^{-1} PCNB in a glass-stoppered Erlenmeyer flask. The initial OD_{600} was 1.8 (a dry weight cell concentration of 0.8 g liter^{-1}). The flask cultures were kept at 37°C and shaken at 210 rpm for 12 h. Triplicate flasks were withdrawn at selected time points, and 20 ml of acetonitrile was added to each, giving a sample solution of 30 ml. Each sample solution was centrifuged at 19,000 $\times$ *g* for 10 min, and the HCB and PCP concentrations in the supernatant were analyzed by HPLC with a photodiode array detector.

The effect of oxygen on HCB degradation activity was investigated using 40-ml aliquots of an isopropyl β-D-1-thiogalactopyranoside-induced cell culture washed with phosphate-buffered saline. The subsequent procedures were performed in a glove box (UN-650F; UNICO, Ibaraki, Japan) with a N_2 atmosphere. Washed cells were suspended in 1 ml of MM that had been purged with N_2 (99.9%) for 20 min to remove dissolved oxygen. The cells were then inoculated into 9 ml of MM containing 4 μmol liter^{-1} HCB in a glass-stoppered Erlenmeyer flask. The initial OD_{600} was 9.0. The oxygen concentration was measured independently using a dissolved oxygen meter (SG6–SevenGo pro dissolved oxygen; Mettler-Toledo, Greifensee, Switzerland). Each culture was kept at room temperature and constantly stirred using a magnetic stirrer, and then after 3 h, oxygen was reintroduced by replacing the N_2 atmosphere with ambient air. Triplicate flasks were withdrawn at specified time points. Control cultures were kept under oxygen-limited conditions ($[O_2] < 0.5$ mg liter^{-1}) throughout the experiment. The samples were prepared and analyzed as described above.

RT-PCR. A single colony of strain PD653 was inoculated into the preculture medium and cultured to the mid-exponential phase ($OD_{600} = 1.0$) at 30°C on a shaker at 180 rpm for 4 days. An aliquot of the culture was inoculated into fresh preculture medium in a glass-stoppered Erlenmeyer flask to give an OD_{600} of 0.1, and then the culture was cultivated. Strain PD653 was grown in the medium, and HCB was added during the exponential phase ($OD_{600} = 0.3$ to 0.4). Cells were harvested after 3 h of incubation and stored at −80°C until use. Total RNA was extracted according to the manufacturer's instructions with some modifications to the initial steps. Briefly, cells were resuspended in 200 μl Tris-EDTA buffer containing 5 mg ml^{-1} lysozyme, the cells were incubated at 37°C for 5 min, and then 500 μl Sepasol-RNA I (Nacalai Tesque, Kyoto, Japan) was added. The sample was placed in a 1.5-ml screw-cap tube containing glass beads (50 mg of beads 100 μm in diameter and 30 mg of beads 1 mm in diameter). The mixture was disrupted using a bead beater at 5,000 rpm for 5 min, and then 500 μl of Sepasol-RNA I was added. DNA traces were removed using total RNA and recombinant DNase (TaKaRa, Tokyo, Japan). The RNA quality was checked by performing 1% native agarose gel electrophoresis. The RNA concentration was determined using a NanoDrop ND-1000 system (Thermo Fisher, Lafayette, CO, USA). cDNA was synthesized from 1 μg total RNA by reverse transcription using a ReverTra Ace quantitative PCR (qPCR) RT kit (Toyobo) following the manufacturer's recommendations. Reverse transcription reaction 8.0 was performed at 37°C for 15 min, 50°C for 15 min, and 98°C for 5 min. The cDNA product was diluted by a factor of eight and then used as the template for RT-PCR analyses using the primers shown in Table 3. The primers used in the RT-PCR process were hcbA1_q_F and hcbA2_q_R for intergenic region I and hcbA2_q_F and hcbA3_q_R for intergenic region II. rpoB_q_R for *rpoB*, a housekeeping gene encoding

the RNA polymerase β-subunit, was used as a positive control in the RT-PCR experiments. The PCR conditions were one cycle at 1.5 min, 30 cycles at 98°C for 15 s, 62.5°C for 30 s, 68°C for 30 s, and finally one cycle at 68°C for 30 s. The PCR products were separated by electrophoresis using 1.5% (wt/vol) agarose gel.

Accession number(s). The strain PD653 and PD653-B2 genome sequences have been deposited in DDBJ/EMBL/GenBank under accession numbers BDJG01000001 to BDJG01000087 and BDJE01000001 to BDJE01000081, respectively.

Strain PD653-B2 was submitted to the Japanese National Agriculture and Food Research Organization GeneBank project (https://www.gene.affrc.go.jp/about_en.php) under MAFF number 304153.

SUPPLEMENTAL MATERIAL

Supplemental material for this article may be found at https://doi.org/10.1128/AEM.00824-17.

SUPPLEMENTAL FILE 1, PDF file, 0.4 MB.

ACKNOWLEDGMENTS

We thank M. Kuramata for help with the experimental design and M. Devers-Lamrani for scientific discussions. We thank Gareth Thomas from Edanz Group for editing a draft of the manuscript.

This work was supported by a grant from the MEXT-Supported Program for the Strategic Research Foundation at Private Universities 2013 to 2017 (grant S1311017) and the Cooperative Research Programme, Trade and Agriculture (TAD/PROG) OECD/2010.

REFERENCES

1. Barber JL, Sweetman AJ, van Wijk D, Jones KC. 2005. Hexachlorobenzene in the global environment: emissions, levels, distribution, trends and processes. Sci Total Environ 349:1–44. https://doi.org/10.1016/j.scitotenv.2005.03.014.
2. Adrian L, Szewzyk U, Wecke J, Görisch H. 2000. Bacterial dehalorespiration with chlorinated benzenes. Nature 408:580–583. https://doi.org/10.1038/35046063.
3. Leys D, Adrian L, Smidt H. 2013. Organohalide respiration: microbes breathing chlorinated molecules. Philos Trans R Soc B Biol Sci 368:20120316. https://doi.org/10.1098/rstb.2012.0316.
4. Jayachandran G, Görisch H, Adrian L. 2003. Dehalorespiration with hexachlorobenzene and pentachlorobenzene by *Dehalococcoides* sp. strain CBDB1. Arch Microbiol 180:411–416. https://doi.org/10.1007/s00203-003-0607-7.
5. Hölscher T, Görisch H, Adrian L. 2003. Reductive dehalogenation of chlorobenzene congeners in cell extracts of *Dehalococcoides* sp. strain CBDB1. Appl Environ Microbiol 69:2999–3001. https://doi.org/10.1128/AEM.69.5.2999-3001.2003.
6. Adrian L, Hansen SK, Fung JM, Görisch H, Zinder SH. 2007. Growth of *Dehalococcoides* strains with chlorophenols as electron acceptors. Environ Sci Technol 41:2318–2323. https://doi.org/10.1021/es062076m.
7. Adrian L, Rahnenführer J, Gobom J, Hölscher T. 2007. Identification of a chlorobenzene reductive dehalogenase in *Dehalococcoides* sp. strain CBDB1. Appl Environ Microbiol 73:7717–7724. https://doi.org/10.1128/AEM.01649-07.
8. Kube M, Beck A, Zinder SH, Kuhl H, Reinhardt R, Adrian L. 2005. Genome sequence of the chlorinated compound-respiring bacterium *Dehalococcoides* species strain CBDB1. Nat Biotechnol 23:1269–1273. https://doi.org/10.1038/nbt1131.
9. Jones JP, O'Hare EJ, Wong LL. 2001. Oxidation of polychlorinated benzenes by genetically engineered CYP101 (cytochrome $P450_{cam}$). Eur J Biochem 268:1460–1467. https://doi.org/10.1046/j.1432-1327.2001.02018.x.
10. Chen X, Christopher A, Jones JP, Bell SG, Guo Q, Xu F, Rao Z, Wong LL. 2002. Crystal structure of the F87W/Y96F/V247L mutant of cytochrome P-450cam with 1,3,5-trichlorobenzene bound and further protein engineering for the oxidation of pentachlorobenzene and hexachlorobenzene. J Biol Chem 277:37519–37526. https://doi.org/10.1074/jbc.M203762200.
11. Yan DZ, Liu H, Zhou NY. 2006. Conversion of *Sphingobium chlorophenolicum* ATCC 39723 to a hexachlorobenzene degrader by metabolic engineering. Appl Environ Microbiol 72:2283–2286. https://doi.org/10.1128/AEM.72.3.2283-2286.2006.
12. Liu T, Chen ZL, Shen YF. 2009. Aerobic biodegradation of hexachlorobenzene by an acclimated microbial community. Int J Environ Pollut 37:235–244. https://doi.org/10.1504/IJEP.2009.025127.
13. Takagi K, Iwasaki A, Kamei I, Satsuma K, Yoshioka Y, Harada N. 2009. Aerobic mineralization of hexachlorobenzene by newly isolated pentachloronitrobenzene-degrading *Nocardioides* sp. strain PD653. Appl Environ Microbiol 75:4452–4458. https://doi.org/10.1128/AEM.02329-08.
14. Apajalahti JHA, Salkinoja-Salonen MS. 1986. Degradation of polychlorinated phenols by *Rhodococcus chlorophenolicus*. Appl Microbiol Biotechnol 25:62–67. https://doi.org/10.1007/BF00252514.
15. Karn SK, Chakrabarti SK, Reddy MS. 2011. Degradation of pentachlorophenol by *Kocuria* sp. CL2 isolated from secondary sludge of pulp and paper mill. Biodegradation 22:63–69. https://doi.org/10.1007/s10532-010-9376-6.
16. Singh S, Chandra R, Patel DK, Rai V. 2007. Isolation and characterization of novel *Serratia marcescens* (AY927692) for pentachlorophenol degradation from pulp and paper mill waste. World J Microbiol Biotechnol 23:1747–1754. https://doi.org/10.1007/s11274-007-9424-5.
17. Sharma A, Thakur IS, Dureja P. 2009. Enrichment, isolation and characterization of pentachlorophenol degrading bacterium *Acinetobacter* sp. ISTPCP-3 from effluent discharge site. Biodegradation 20:643–650.
18. Lee SG, Yoon BD, Park YH, Oh HM. 1998. Isolation of a novel pentachlorophenol-degrading bacterium, *Pseudomonas* sp. Bu34. J Appl Microbiol 85:1–8. https://doi.org/10.1046/j.1365-2672.1998.00456.x.
19. Cai M, Xun L. 2002. Organization and regulation of pentachlorophenol-degrading genes in *Sphingobium chlorophenolicum* ATCC 39723. J Bacteriol 184:4672–4680. https://doi.org/10.1128/JB.184.17.4672-4680.2002.
20. Darling AC, Mau B, Blattner FR, Perna NT. 2004. Mauve: multiple alignment of conserved genomic sequence with rearrangements. Genome Res 14:1394–1403. https://doi.org/10.1101/gr.2289704.
21. Gisi MR, Xun L. 2003. Characterization of chlorophenol 4-monooxygenase (TftD) and NADH:flavin adenine dinucleotide oxidoreductase (TftC) of *Burkholderia cepacia* AC1100. J Bacteriol 185:2786–2792. https://doi.org/10.1128/JB.185.9.2786-2792.2003.
22. Perkins EJ, Gordon MP, Caceres O, Lurquin PF. 1990. Organization and sequence analysis of the 2,4-dichlorophenol hydroxylase and dichlorocatechol oxidative operons of plasmid pJP4. J Bacteriol 172:2351–2359. https://doi.org/10.1128/jb.172.5.2351-2359.1990.
23. Seibert V, Stadler-Fritzsche K, Schlömann M. 1993. Purification and characterization of maleylacetate reductase from *Alcaligenes eutrophus* JMP134(pJP4). J Bacteriol 175:6745–6754. https://doi.org/10.1128/jb.175.21.6745-6754.1993.

24. Strohl WR. 1992. Compilation and analysis of DNA sequences associated with apparent streptomycete promoters. Nucleic Acids Res 20:961–974. https://doi.org/10.1093/nar/20.5.961.
25. Vögtli M, Hütter R. 1987. Characterization of the hydroxystreptomycin phosphotransferase gene (*sph*) of *Streptomyces glaucescens*: nucleotide sequence and promoter analysis. Mol Gen Genet 208:195–203. https://doi.org/10.1007/BF00330442.
26. Weir KM, Sutherland TD, Horne I, Russell RJ, Oakeshott JG. 2006. A single monooxygenase, *ese*, is involved in the metabolism of the organochlorides endosulfan and endosulfate in an *Arthrobacter* sp. Appl Environ Microbiol 72:3524–3530. https://doi.org/10.1128/AEM.72.5.3524-3530.2006.
27. Bohuslavek J, Payne JW, Liu Y, Bolton H, Xun L. 2001. Cloning, sequencing, and characterization of a gene cluster involved in EDTA degradation from the bacterium BNC1. Appl Environ Microbiol 67:688–695. https://doi.org/10.1128/AEM.67.2.688-695.2001.
28. Takagi K, Yoshioka Y, Iwasaki A, Kamei I, Harada N. 2007. Metabolic pathways of hexachlorobenzene (HCB), quintozene (PCNB) and pentachlorophenol (PCP) by a newly isolated strain *Nocardioides* sp. PD653 under aerobic conditions. Organohalogen Compd 69:2576–2579.
29. Siguier P, Filée J, Chandler M. 2006. Insertion sequences in prokaryotic genomes. Curr Opin Microbiol 9:526–531. https://doi.org/10.1016/j.mib.2006.08.005.
30. Ghisla S, Massey V. 1989. Mechanisms of flavoprotein-catalyzed reactions. Eur J Biochem 181:1–17. https://doi.org/10.1111/j.1432-1033.1989.tb14688.x.
31. Huijbersa MME, Montersinoa S, Westphala AH, Tischlera D, van Berkela WJH. 2014. Flavin dependent monooxygenases. Arch Biochem Biophys 544:2–17. https://doi.org/10.1016/j.abb.2013.12.005.
32. Feng L, Wang W, Cheng J, Ren Y, Zhao G, Gao C, Tang Y, Liu X, Han W, Peng X, Liu R, Wang L. 2007. Genome and proteome of long-chain alkane degrading *Geobacillus thermodenitrificans* NG80-2 isolated from a deep-subsurface oil reservoir. Proc Natl Acad Sci U S A 104:5602–5607. https://doi.org/10.1073/pnas.0609650104.
33. Li L, Liu X, Yang W, Xu F, Wang W, Feng L, Bartlam M, Wang L, Rao Z. 2008. Crystal structure of long-chain alkane monooxygenase (LadA) in complex with coenzyme FMN: unveiling the long-chain alkane hydroxylase. J Mol Biol 376:453–465. https://doi.org/10.1016/j.jmb.2007.11.069.
34. Eichhorn E, Davey CA, Sargent DF, Leisinger T, Richmond TJ. 2002. Crystal structure of *Escherichia coli* alkanesulfonate monooxygenase SsuD. J Mol Biol 324:457–468. https://doi.org/10.1016/S0022-2836(02)01069-0.
35. Fisher AJ, Thompson TB, Thoden JB, Baldwin TO, Rayment I. 1996. The 1.5-Å resolution crystal structure of bacterial luciferase in low salt conditions. J Biol Chem 271:21956–21968. https://doi.org/10.1074/jbc.271.36.21956.
36. Aufhammer SW, Warkentin E, Berk H, Shima S, Thauer RK, Ermler U. 2004. Coenzyme binding in F_{420}-dependent secondary alcohol dehydrogenase, a member of the bacterial luciferase family. Structure 12:361–370. https://doi.org/10.1016/j.str.2004.02.010.
37. Shima S, Warkentin E, Grabarse W, Sordel M, Wicke M, Thauer RK, Ermler U. 2000. Structure of coenzyme F_{420} dependent methylenetetrahydromethanopterin reductase from two methanogenic archaea. J Mol Biol 300:935–950. https://doi.org/10.1006/jmbi.2000.3909.
38. Moore SA, James MNG. 1994. Common structural features of the LuxF protein and the subunits of bacterial luciferase: evidence for a ($\beta\alpha$)8 fold in luciferase. Protein Sci 3:1914–1926. https://doi.org/10.1002/pro.5560031103.
39. Xun L. 1996. Purification and characterization of chlorophenol 4-monooxygenase from *Burkholderia cepacia* AC1100. J Bacteriol 178:2645–2649. https://doi.org/10.1128/jb.178.9.2645-2649.1996.
40. Duffner FM, Mueller R. 1998. A novel phenol hydroxylase and catechol 2,3-dioxygenase from the thermophilic *Bacillus thermoleovorans* strain A2: nucleotide sequence and analysis of the genes. FEMS Microbiol Lett 161:37–45. https://doi.org/10.1111/j.1574-6968.1998.tb12926.x.
41. Prieto MA, Perez-Aranda A, Garcia JL. 1993. Characterization of an *Escherichia coli* aromatic hydroxylase with a broad substrate range. J Bacteriol 175:2162–2167. https://doi.org/10.1128/jb.175.7.2162-2167.1993.
42. Kirchner U, Westphal AH, Müller R, van Berkel WJH. 2003. Phenol hydroxylase from *Bacillus thermoglucosidasius* A7, a two-protein component monooxygenase with a dual role for FAD. J Biol Chem 278:47545–47553. https://doi.org/10.1074/jbc.M307397200.
43. Galán B, Díaz E, Prieto MA, García JL. 2000. Functional analysis of the small component of the 4-hydroxyphenylacetate 3-monooxygenase of *Escherichia coli* W: a prototype of a new flavin:NAD(P)H reductase subfamily. J Bacteriol 182:627–636. https://doi.org/10.1128/JB.182.3.627-636.2000.
44. Spanjaard RA, van Duin J. 1989. Translational reinitiation in the presence and absence of a Shine and Dalgarno sequence. Nucleic Acids Res 17:5501–5507. https://doi.org/10.1093/nar/17.14.5501.
45. Sprengel R, Reiss B, Schaller H. 1985. Translationally coupled initiation of protein synthesis in *Bacillus subtilis*. Nucleic Acids Res 13:893–909. https://doi.org/10.1093/nar/13.3.893.
46. Adhin MR, van Duin J. 1990. Scanning model for translational reinitiation in eubacteria. J Mol Biol 213:811–818. https://doi.org/10.1016/S0022-2836(05)80265-7.
47. Yoo JH, RajBhandary UR. 2008. Requirements for translation re-initiation in *Escherichia coli*: roles of initiator tRNA and initiation factors IF2 and IF3. Mol Microbiol 67:1012–1026. https://doi.org/10.1111/j.1365-2958.2008.06104.x.
48. Whyte LG, Smits THM, Labbé D, Witholt B, Greer CW, van Beilen JB. 2002. Gene cloning and characterization of multiple alkane hydroxylase systems in *Rhodococcus* strains Q15 and NRRL B-16531. Appl Environ Microbiol 68:5933–5942. https://doi.org/10.1128/AEM.68.12.5933-5942.2002.
49. Nagy I, Schoofs G, Compernolle F, Proost P, Vanderleyden J, De Mot R. 1995. Degradation of the thiocarbamate herbicide EPTC (S-ethyl dipropylcarbamothioate) and biosafening by *Rhodococcus* sp. strain NI86/21 involve an inducible cytochrome P-450 system and aldehyde dehydrogenase. J Bacteriol 177:676–687. https://doi.org/10.1128/jb.177.3.676-687.1995.
50. Mattes TE, Coleman NV, Spain JC, Gossett JM. 2005. Physiological and molecular genetic analyses of vinyl chloride and ethene biodegradation in *Nocardioides* sp. strain JS614. Arch Microbiol 183:95–106. https://doi.org/10.1007/s00203-004-0749-2.
51. Yamazaki K, Fujii K, Iwasaki A, Takagi K, Satsuma K, Harada N, Uchimura T. 2008. Different substrate specificities of two triazine hydrolases (TrzNs) from *Nocardioides* species. FEMS Microbiol Lett 286:171–177. https://doi.org/10.1111/j.1574-6968.2008.01271.x.
52. Yanze-Kontchou C, Gschwind N. 1994. Mineralization of the herbicide atrazine as a carbon source by a *Pseudomonas* strain. Appl Environ Microbiol 60:4297–4302.
53. Assefa S, Keane TM, Otto TD, Newbold C, Berriman M. 2009. ABACAS: algorithm-based automatic contiguation of assembled sequences. Bioinformatics 25:1968–1969. https://doi.org/10.1093/bioinformatics/btp347.
54. Ellis LBM, Wackett LP. 2012. Use of the University of Minnesota Biocatalysis/Biodegradation Database for study of microbial degradation. Microb Inform Exp 2:1. https://doi.org/10.1186/2042-5783-2-1.
55. Drozdetskiy A, Cole C, Procter J, Barton GJ. 2015. JPred4: a protein secondary structure prediction server. Nucleic Acids Res 43:W389–W394. https://doi.org/10.1093/nar/gkv332.